Comparison of Dorsocervical With Abdominal Subcutaneous Adipose Tissue in Patients With and Without Antiretroviral Therapy–Associated Lipodystrophy

Ksenia Sevastianova,[1,2] Jussi Sutinen,[2,3] Dario Greco,[4] Meline Sievers,[5] Kaisa Salmenkivi,[6] Julia Perttilä,[1] Vesa M. Olkkonen,[1] Dick Wågsäter,[7] Martin E. Lidell,[8] Sven Enerbäck,[8] Per Eriksson,[7] Ulrich A. Walker,[9] Petri Auvinen,[4] Matti Ristola,[3] and Hannele Yki-Järvinen[2]

OBJECTIVE—Combination antiretroviral therapy (cART) is associated with lipodystrophy, i.e., loss of subcutaneous adipose tissue in the abdomen, limbs, and face and its accumulation intra-abdominally. No fat is lost dorsocervically and it can even accumulate in this region (buffalo hump). It is unknown how preserved dorsocervical fat differs from abdominal subcutaneous fat in HIV-1–infected cART-treated patients with (cART+LD+) and without (cART+LD−) lipodystrophy.

RESEARCH DESIGN AND METHODS—We used histology, microarray, PCR, and magnetic resonance imaging to compare dorsocervical and abdominal subcutaneous adipose tissue in cART+LD+ (n = 21) and cART+LD− (n = 11).

RESULTS—Albeit dorsocervical adipose tissue in cART+LD+ seems spared from lipoatrophy, its mitochondrial DNA (mtDNA; copies/cell) content was significantly lower (by 62%) than that of the corresponding tissue in cART+LD−. Expression of CD68 mRNA, a marker of macrophages, and numerous inflammatory genes in microarray were significantly lower in dorsocervical versus abdominal subcutaneous adipose tissue. Genes with the greatest difference in expression between the two depots were those involved in regulation of transcription and regionalization (homeobox genes), irrespective of lipodystrophy status. There was negligible mRNA expression of uncoupling protein 1, a gene characteristic of brown adipose tissue, in either depot.

CONCLUSIONS—Because mtDNA is depleted even in the nonatrophic dorsocervical adipose tissue, it is unlikely that the cause of lipoatrophy is loss of mtDNA. Dorsocervical adipose tissue is less inflamed than lipoatrophic adipose tissue. It does not resemble brown adipose tissue. The greatest difference in gene expression between dorsocervical and abdominal subcutaneous adipose tissue is in expression of homeobox genes.
Diabetes **60:1894–1900, 2011**

From the [1]Minerva Institute for Medical Research, Helsinki, Finland; the [2]Department of Medicine, Division of Diabetes, Helsinki University Central Hospital, Helsinki, Finland; the [3]Department of Medicine, Division of Infectious Diseases, Helsinki University Central Hospital, Helsinki, Finland; the [4]Institute of Biotechnology, University of Helsinki, Helsinki, Finland; the [5]Department of Rheumatology and Clinical Immunology, Medizinische Universitätsklinik, Freiburg, Germany; the [6]Department of Pathology, Helsinki University Central Hospital, Helsinki, Finland; the [7]Center for Molecular Medicine and Department of Medicine, Karolinska University Hospital, Karolinska Institute, Stockholm, Sweden; the [8]Department of Medical and Clinical Genetics, University of Gothenburg, Gothenburg, Sweden; and the [9]Department of Rheumatology, University of Basel, Basel, Switzerland.

Corresponding author: Ksenia Sevastianova, ksenia.sevastianova@helsinki.fi.
Received 20 January 2011 and accepted 19 April 2011.

DOI: 10.2337/db11-0075

This article contains Supplementary Data online at http://diabetes.diabetesjournals.org/lookup/suppl/doi:10.2337/db11-0075/-/DC1.

Use of combination antiretroviral therapy (cART) is associated with the lipodystrophy syndrome, which is characterized by loss of adipose tissue (lipoatrophy) in face, limbs, and abdominal subcutaneous region and accumulation of adipose tissue (lipohypertrophy) intra-abdominally and subcutaneously in the dorsocervical upper trunk (buffalo hump) (1). Although lipoatrophy has been extensively studied both in vitro and in vivo (2–4), lipohypertrophy is poorly understood. There are no data comparing dorsocervical adipose tissue (hypertrophic depot) to abdominal subcutaneous adipose tissue (lipoatrophic depot) from the same individuals and no existing in vitro models explaining their opposite pathophysiology.

There are some but sparse clinical observational data regarding the buffalo hump. The prevalence of buffalo hump, as determined by physical examination, has been estimated to be 2–13% in all HIV-1–infected cART-treated patients and up to 25% in those with the lipodystrophy syndrome (5). In a large group of lipodystrophic patients (n = 417), the presence as compared with the absence of buffalo hump was associated with higher prevalence of visceral adiposity and features of insulin resistance such as fasting serum insulin, C-peptide, and homeostasis model assessment of insulin resistance (HOMA-IR) (5). In a study comparing 926 HIV-1–positive (lipodystrophy status not specified) with 258 HIV-1–negative subjects, upper trunk subcutaneous adipose tissue (on both chest and neck, measured by magnetic resonance imaging [MRI]) was shown to be associated with insulin resistance as measured by HOMA-IR independent of obesity parameters other than intra-abdominal fat (6). In HIV-1–negative subjects, accumulation of dorsocervical adipose tissue has been associated with general and visceral obesity as well as other features of the metabolic syndrome (7–9). Thus the buffalo hump associated with the lipodystrophy syndrome may provide an interesting model of hypertrophic adipose tissue in humans.

It is unclear why in HIV-1–infected cART-treated patients adipose tissue remains normal or even hypertrophies in some areas (e.g., dorsocervically), whereas it atrophies in others (e.g., abdominal subcutis and limbs). In mice, interscapular adipose tissue is known to be brown adipose tissue (BAT) (10). BAT, as opposed to white adipose tissue, is exceptionally rich in mitochondria (11). BAT mitochondria express exceptionally high amounts of

uncoupling protein 1 (UCP1) (12), a protein responsive for the main function of BAT: adaptive thermogenesis (13). Identification of *UCP1* mRNA in dorsocervical adipose tissue of patients with the lipodystrophy syndrome (14,15) has evoked a hypothesis that buffalo hump might be metabolically active BAT. However, after completion of the current study, positron emission tomography (PET) studies have demonstrated that BAT in healthy humans is localized in supraclavicular rather than dorsocervical region (16–18). PET studies have not found BAT in subjects with the lipodystrophy syndrome (19).

In the current study, we compared characteristics of the dorsocervical and the abdominal subcutaneous adipose tissue from the same individuals in a group of 32 cART-treated patients with and without lipodystrophy using histology, microarray, real-time PCR, and MRI.

RESEARCH DESIGN AND METHODS

Study subjects. After approval of the study protocol by the appropriate Ethics Committee, 32 study subjects were recruited from the HIV outpatient clinic of the Helsinki University Central Hospital. All were required to have been on cART for at least 18 months with unchanged regimen for at least 12 weeks before the study. The purpose, nature, and potential risks of the study were explained to the patients, and their written informed consent was obtained. The participants were subgrouped according to the presence or absence of lipodystrophy. Lipodystrophy was determined as self-reported and investigator-confirmed (J.S.) loss of subcutaneous adipose tissue with or without accumulation of adipose tissue intra-abdominally or in the dorsocervical upper trunk. Subjects fulfilling these criteria were included in the lipodystrophic study group (cART+LD+; $n = 21$). Subjects without lipodystrophy (cART+LD−; $n = 11$) had received cART without developing the aforementioned changes in body fat composition. Pregnancy and signs, symptoms, or biochemical evidence of active diseases other than HIV-1 were exclusion criteria. All subjects were studied after an overnight fast. The study subjects had participated previously in a study comparing expression of selected genes in abdominal subcutaneous adipose tissue between lipoatrophic and nonlipoatrophic patients (20). The lipoatrophic patients have also participated in a clinical treatment trial with uridine (21). All present data on dorsocervical adipose tissue as well as microarray and histology data from both dorsocervical and abdominal subcutaneous adipose tissue are novel.

Surgical subcutaneous adipose tissue biopsies. After local anesthesia with lidocaine, surgical subcutaneous adipose tissue biopsies were taken from the midway between the iliac crest and the umbilicus as well as from the midline at the base of the neck. Part of the biopsy was immediately snap-frozen in liquid nitrogen, whereas another part was formalin-fixed and paraffin-embedded for subsequent histological analyses.

Analysis of adipose tissue biopsies

Mitochondrial DNA copy numbers. Genomic DNA was extracted from adipose tissue with the QIAamp DNA isolation kit (Qiagen, Hilden, Germany). Mitochondrial DNA (mtDNA) and nuclear DNA (nDNA) copy numbers were determined by quantitative PCR using the ABI 7700 sequence detection system (Applied Biosystems, Foster City, CA). All samples were run in triplicate. Absolute mtDNA and nDNA copy numbers were calculated using serial dilutions of plasmids with known copy numbers. Details on primers and exact PCR methodology have been published previously (20).

Light microscopy. Formalin-fixed, paraffin-embedded subcutaneous adipose tissue samples were sectioned using a standard protocol. The slides were stained with hematoxylin and eosin and examined under the light microscope (Nikon Eclipse 80i; Nikon Corporation, Tokyo, Japan) for the amount of connective tissue; vascularization; lipogranulomata, i.e., lipid-laden macrophages encircling adipocytes; degree of adipocyte size variation; and the presence of cell membrane rupture and brown adipocytes. Images for publication were taken using the computer software compatible with the microscope (NIS-Elements 3.0; Nikon Corporation).

RNA extraction. Adipose tissue per patient (100 mg) was homogenized using the isolation kit Geneclean (Bio101 systems; Obiogene, Carlsbad, CA). RNA was extracted with the RNeasy Lipid Tissue Kit (Qiagen, Hilden, Germany) following the manufacturer's instructions. Quantity and integrity of RNA were verified using RNA 6000 nanochips (Agilent 2100 Bioanalyser; Palo Alto, CA). Part of the isolated RNA was stored at −80°C until quantification of the target mRNAs by microarray. In addition, of each sample 1.5 μg of RNA were used for reverse transcription using 400U of Superscript II (Invitrogen, Carlsbad, CA) and 100 μM of oligo(dT)$_{12–18}$ (Invitrogen) as primer. Another 0.5 μg of RNA was reverse transcribed using the SuperScript VILO cDNA synthesis kit (Invitrogen).

Microarray. Total RNA (1 μg/sample) was indirectly labeled using the T7 amplification method (Amino Allyl MessageAmpTM II aRNA Amplification Kit; Ambion, Austin, TX) according to the manufacturer's instructions. The amplified RNA (aRNA; 5 μg/sample) was labeled using monoreactive Cy3 or Cy5 dyes (GE Healthcare, GE Life Sciences, Uppsala, Sweden) followed by purification according to the manufacturer's instructions. Labeled aRNAs were hybridized onto Whole Human Genome 4 × 44 K microarrays (Agilent Technologies, Santa Clara, CA) according to the manufacturer's instructions. The slides were then washed according to the instructions with buffers from Agilent and scanned with GenePix 4200 AL (Axon Instruments, Molecular Devices, Silicon Valley, CA) at the resolution of 5 μm/pixel and at 16 bit depth. Microarrays were technically unsuccessful in four samples and these patients (all cART+LD+), consequently, were excluded from further analyses. Microarray results were analyzed using Benjamini and Hochberg post hoc correction for multiple comparisons with statistical significance set to $P \leq 0.01$. The analysis was carried out as comparison of dorsocervical to the abdominal subcutaneous adipose tissue in the cART+LD+ and the cART+LD− group separately. DAVID Bioinformatics Resources 6.7 (http://david.abcc.ncifcrf.gov) was used to select over-represented pathways and gene categories (22).

Real-time quantification of gene expression. PCR of *CD68* was carried out on a LightCycler 480 (Roche, Penzberg, Germany) using SYBR-Green technology by Roche as described previously (20). Expression of *CD68* was normalized to the mean of three housekeeping genes (actin β, *ACTB*; acidic ribosomal protein P0, *36B4*; β_2-microglobulin, *B2M*) commonly used (23). The PCR for *UCP1* was carried out in a subset of samples ($n = 6$) from individuals with the clinically largest buffalo humps using ABI PRISM 7900HT instrument and software (PE Applied Biosystems, Foster City, CA) using Power SYBR Green PCR Master Mix (PE Applied Biosystems). Expression of *UCP1* was normalized to *ACTB*. Expression of the homeobox genes (*HOXA10*, *HOXC9*, *HOXC8*, and *SHOX2*) chosen to verify the microarray results was measured using SYBR-Green kit according to the manufacturer's protocol on ABI PRISM 7000 Sequence Detection System instrument and software (PE Applied Biosystems). Expression of homeobox genes was normalized to *36B4*. All samples were run in duplicates, and the results were calculated from the real-time PCR efficiency (24). Primers used for PCR analyses are given in Table 1.

Measures of body composition. Body circumferences were measured in triplicates with a nonstretchable band for the waist midway between the lower rib margin and the iliac crest and, for the hip circumference, over the greater trochanters and recorded to the nearest 0.5 cm. Skinfold thickness (mean values of triplicate measurements) was determined at five sites (triceps, biceps, iliac crest, thigh, and scapula) (25). Limb, trunk, and total body fat were measured using dual-energy X-ray absorptiometry (DEXA; Lunar Prodigy, Madison, WI). Intra-abdominal fat as well as abdominal and dorsocervical subcutaneous fat were quantified by analyzing T1-weighted two-dimensional fast low angle shot *trans*-axial MRI scans. Details for image acquisition for intra-abdominal and abdominal subcutaneous fat have been given previously (26). Dorsocervical subcutaneous fat volume was measured from scans acquired by the methodology described above covering the area between second and third cervical vertebra to the lower edge of scapula (slice thickness, 5 mm; field of view, 315 × 500 mm^2; time of repetition, 159 ms; echo time, 4.1 ms). Liver fat content was measured using proton magnetic resonance spectroscopy, as previously described (27).

Analytical procedures. Plasma glucose concentrations were measured using a hexokinase method, serum total, and HDL cholesterol and triglyceride concentrations with respective enzymatic kits from Roche Diagnostics using an autoanalyzer (Roche Diagnostics, Hitachi 917; Hitachi, Tokyo, Japan). The concentration of LDL cholesterol was calculated using the formula of Friedewald et al. (28). Serum insulin and C-peptide concentrations were determinedby time-resolved fluoroimmunoassay using Insulin and C-peptide Kits (AUTOdelfia, Wallac, Turku, Finland), respectively. HOMA-IR was calculated from the formula: fasting glucose (mmol/L) × fasting insulin (mU/L)/22.5 (29). Serum ALT activity was determined as recommended by the European Committee for Clinical Laboratory Standards. Serum C-reactive protein (CRP) was analyzed using a commercial kit (Ultrasensitive CRP Kit; Orion Diagnostica, Espoo, Finland). CD4+ T-cell count was determined using flow-cytometry (FACSort/FACSCalibur; Becton Dickinson, San José, CA). HIV-1 viral load was measured using HPS Cobas TaqMan 48n HIV-1 Test (Roche Diagnostics, Branchburg, NJ) with a detection limit of 50 copies/mL. Shygmomanometric measurement of brachial pressure was conducted after a minimum of 15 min of acclimatization and before blood sampling.

Statistics. Demographic and clinical parameters among the study groups were compared using Fisher exact test or χ^2 test for categorical variables and unpaired *t* test or Mann-Whitney test for continuous variables, as appropriate. Distribution was tested for normality using a Kolmogorov-Smornov test. Wilcoxon matched pairs test was used to compare intraindividual data.

TABLE 1
Primers used for mRNA analyses

Gene	Forward primer 5′–3′	Backward primer 5′–3′
*36B4**	CTGGAAAACAACCCAGCTCT	GAACACAAAGCCCACATTCC
36B4†	CATGCTCAACATCTCCCCCTTCTCC	GGGAAGGTGTAATCCGTCTCCACAG
*ACTB**	ATTGGCAATGAGCGGTTC	GGATGCCACAGGACTCCAT
ACTB‡	GAGCTACGAGCTGCCTGACG	GTAGTTTCGTGGATGCCACAG
B2M	TTCTGGCCTGGAGGCTATC	TCAGGAAATTTGACTTTCCATTC
CD68	GAATTTTATTAAATGTGACGAACTGC	GGAAAACCCCGTCAAAGATT
UCP1	CTGGAATAGCGGCGTGCTT	AATAACACTGGACGTCGGGC
SHOX2	TGTTCGTGTGGATGCACGTG	GAAACCAAACCTGCACTCGG
HOXA10	GAGAGCAGCAAAGCCTCGC	CCAGTGTCTGGTGCTTCGTG
HOXC9	GCCTGCTGCCTCAGCACAG	GAACCCTCCCAAATCGCAAG
HOXC8	TCTCCAACTCAGGCTACCAG	TGAGCCCCATAAAGGGACTGT

*Used as a housekeeping gene in *CD68* expression analysis; †used as a housekeeping gene in homeobox gene expression analysis; ‡used as a housekeeping gene in *UCP1* expression analysis.

Correlations were calculated using Spearman rank correlation coefficient. For statistical analyses GraphPad Prism version 4 (GraphPad Software, San Diego, CA) and Lotus 1-2-3 of Lotus SmartSuite Release 9.5 (Lotus Development Corporation, IBM Corporation, New York, NY) were used. Data are given as mean ± SEM or median (25% percentile–75% percentile), as appropriate. Two-tailed P values < 0.05 were considered statistically significant. Statistical analyses of the microarray data are described in detail above.

RESULTS

Study subjects. Characteristics of the patients are given in Table 2. The cART+LD+ and the cART+LD− groups were comparable with respect to age, sex, and BMI. The cART+LD+ group had significantly higher ratios of dorsocervical to abdominal subcutaneous and intra-abdominal to abdominal subcutaneous adipose tissue than the cART+LD− group. Serum insulin, HOMA-IR, and triglyceride concentrations were significantly higher and HDL cholesterol concentrations lower in the cART+LD+ compared with the cART+LD− group (Table 2).

Analysis of adipose tissue biopsies

mtDNA copy numbers: dorsocervical versus abdominal subcutaneous adipose tissue. The mtDNA copy number was significantly higher in the dorsocervical than in the abdominal subcutaneous adipose tissue in the cART+LD+ group (356 ± 59 vs. 256 ± 44 copies/cell; $P = 0.01$). A similar trend was found in the cART+LD− group (930 ± 109 vs. 563 ± 161 copies/cell; $P = 0.08$; Fig. 1).

mtDNA copy numbers: cART+LD+ versus cART+LD−. The mtDNA copy number was 62% lower in the cART+LD+ than in the cART+LD− group in the dorsocervical ($P < 0.0001$) and 54% lower in the abdominal subcutaneous adipose tissue ($P = 0.03$; Fig. 1).

Light microscopy: dorsocervical versus abdominal subcutaneous adipose tissue. The dorsocervical adipose tissue in both the cART+LD+ and the cART+LD− group had significantly less adipocytes (55 ± 6 vs. 77 ± 5%, $P = 0.01$; and 61 ± 5 vs. 89 ± 4%, $P < 0.00001$, respectively) and more connective tissue (45 ± 6 vs. 23 ± 5%, $P = 0.01$; and 39 ± 5 vs. 11 ± 4%, $P < 0.00001$, respectively) than the abdominal subcutaneous adipose tissue (Fig. 2). The two depots were similar with respect to variation in adipocyte size, cell membrane rupture, presence of lipogranulomata, and cells morphologically typical to BAT irrespective of the lipodystrophy status (data not shown).

Light microscopy: cART+LD+ versus cART+LD−. The abdominal subcutaneous adipose tissue from patients in the cART+LD+ group contained significantly more lipogranulomata ($P = 0.045$) than the corresponding tissue from the cART+LD− group (Fig. 2). Other histological parameters did not differ significantly between the cART+LD+ and the cART+LD− group in either depot.

Microarray: dorsocervical versus abdominal subcutaneous adipose tissue in cART+LD+. Microarray analysis comparing the dorsocervical to the abdominal subcutaneous adipose tissue within the cART+LD+ group identified 27,819 probes for genes of which 99 were differentially expressed. These 99 probes corresponded to 75 unique Entrez gene IDs. Of these 75 genes, 61 were dowregulated and 14 upregulated in the dorsocervical compared with the abdominal subcutaneous adipose tissue (Supplementary Table 1; full microarray data are available at Gene Expression Omnibus [GEO], http://www.ncbi.nlm.nih.gov/geo/; accession number GSE28073). The differentially expressed genes were involved in regulation of gene transcription; organ development; and regionalization, immune response, and inflammation as well as in composition and organization of extracellular matrix and cytoskeleton. Three of the top six genes downregulated in the dorsocervical adipose tissue were homeobox genes *HOXA10*, *HOXC9*, and *HOXC8*. These genes are known to be transcription factors providing cells with specific positional identities on the anterior-posterior axis. Among genes upregulated in the dorsocervical compared with the abdominal subcutaneous adipose tissue was short stature homeobox 2 (*SHOX2*), a gene responsible for cranio-facial lateralization of the embryonic cells.

Microarray: dorsocervical versus abdominal subcutaneous adipose tissue in cART+LD−. Microarray analysis comparing the dorsocervical to the abdominal subcutaneous adipose tissue within the cART+LD− group identified 27,900 probes for genes of which 18 were differentially expressed. Of these, 13 corresponded to unique Entrez Gene IDs. Of these 13 genes, 9 were downregulated and 4 upregulated in the dorsocervical compared with the abdominal subcutaneous adipose tissue (Supplementary Table 2; full microarray data are available at GEO, *vide supra*). The differentially expressed genes were involved in regulation of transcription, organ development, and regionalization. The top three downregulated genes were the same *HOXA10*, *HOXC9*, and *HOXC8* genes as in the cART+LD+ group. Also alike in the cART+LD+ group, *SHOX2* was among the genes most upregulated in the dorsocervical as compared with the abdominal adipose tissue.

TABLE 2
Characteristics of the study groups

	cART+LD+	cART+LD−	*P* value
Men/women	18/3	10/1	0.67
Age	47 ± 2	44 ± 3	0.28
Body composition			
Weight (kg)	74 ± 3	75 ± 3	0.72
BMI (kg/m^2)	23.6 ± 0.7	23.7 ± 0.8	0.92
Waist-to-hip ratio	1.00 ± 0.01	0.92 ± 0.02	<0.01
Sum of four skinfolds (mm)*	20 ± 2	28 ± 3	<0.05
Scapular skinfold (mm)	21 ± 3	15 ± 2	0.12
Scapular skinfold/sum of four skinfolds*	1.0 ± 0.1	0.6 ± 0.1	<0.01
Dorsocervical/abdominal subcutaneous adipose tissue volume	1.0 ± 0.1	0.5 ± 0.6	<0.05
Intra-abdominal/abdominal subcutaneous adipose tissue volume	2.3 (0.8–4.5)	0.5 (0.5–0.7)	<0.001
Liver fat (%)	3 (1.5–11.3)	1 (0.75–1.5)	<0.001
Leg fat (g)	1,880 ± 370	4,270 ± 620	<0.01
Limb fat of total fat (%)	20 ± 2	37 ± 1	<0.001
Trunk fat (g)	9,360 ± 1,030	9,380 ± 1,450	0.99
Trunk fat of total fat (%)	76 ± 2	59 ± 1	<0.001
Total body fat (%)	17 ± 2	21 ± 3	0.24
Features of insulin resistance			
Plasma glucose (mmol/L)	5.1 (4.9–5.7)	5.3 (5.1–5.8)	0.28
Serum insulin (mU/L)	12.8 ± 2.4	4.9 ± 0.5	<0.05
Serum C-peptide (nmol/L)	0.85 ± 0.09	0.54 ± 0.06	<0.05
HOMA-IR index	2.3 (1.3–4.1)	1.0 (0.9–1.5)	<0.05
Serum HDL cholesterol (mmol/L)	1.2 ± 0.1	1.8 ± 0.1	<0.001
Serum LDL cholesterol (mmol/L)	2.7 ± 0.2	2.4 ± 0.3	0.39
Serum triglycerides (mmol/L)	3.4 ± 0.5	1.6 ± 0.3	<0.05
Serum hs-CRP (mg/L)	1.6 ± 0.3	0.7 ± 0.2	0.08
Serum ALT (units/L)	38 ± 6	28 ± 4	0.26
Systolic blood pressure (mmHg)	129 ± 3	123 ± 4	0.21
Diastolic blood pressure (mmHg)	81 ± 2	77 ± 3	0.28
HIV-related characteristics			
Time since HIV-1 diagnosis (years)	9.1 ± 1.0	7.8 ± 1.3	0.28
Duration of cART (years)	5.9 ± 0.4	3.8 ± 0.5	<0.01
Patients with undetectable HIV-1 viral load	18/21	11/11	0.53
Most recent CD4+ T-cell count (cells/mm^3)	545 ± 57	522 ± 44	0.79
Current NRTI (%)	100	100	NA
Current NNRTI (%)	20	80	<0.01
Current PI (%)	95	20	<0.001

Data are shown as mean ± SEM or median (25% percentile–75% percentile). ALT, alanine aminotransferase; hs-CRP, highly sensitive C-reactive protein; NA, not applicable; NRTI, nucleoside analog reverse transcriptase inhibitor; NNRTI, nonnucleoside analog reverse transcriptase inhibitor; PI, protease inhibitor. HOMA-IR calculated from the formula: fasting glucose (mmol/L) × fasting insulin (mU/L)/22.5 (29). The concentration of LDL cholesterol was calculated using the formula of Friedewald (28). *The four sites for skinfold thickness measurement, representing the lipoatrophic body parts, were: triceps, biceps, iliac crest, and thigh.

Real-time PCR verification of the microarray data: quantification of expression of homeobox genes in dorsocervical versus abdominal subcutaneous adipose tissue. Expression of *SHOX2* was fourfold higher in the dorsocervical compared with the abdominal subcutaneous adipose tissue in the cART+LD+ and sixfold higher for the respective comparison in the cART+LD− group. Expression of *HOXA10*, *HOXC9*, and *HOXC8* was 18-, 8-, and 11-fold lower in the dorsocervical compared with the abdominal subcutaneous adipose tissue in the cART+LD+ group. In the cART+LD− group, expression of *HOXA10*, *HOXC9*, and *HOXC8* were 21-, 9-, and 10-fold lower in the dorsocervical than in the abdominal subcutaneous adipose tissue. Fold change differences for any of the homeobox genes analyzed were not significantly different between the cART+LD+ and the cART+LD− groups (Fig. 3).

Real-time PCR verification of the microarray data: expression of* UCP1 *in dorsocervical versus abdominal subcutaneous adipose tissue. *UCP1* mRNA was detected in similar minute quantities in some dorsocervical and abdominal subcutaneous adipose tissue samples, but expression was approximately 1,000 times lower than that measured by the same laboratory in human BAT (data not shown) (18).

Real-time PCR verification of the microarray data: expression of* CD68 *mRNA. Expression of *CD68* mRNA, used as a marker of macrophages and, thus, inflammation, was significantly lower in the dorsocervical as compared with the abdominal subcutaneous adipose tissue in the cART+LD+ group (0.39 [0.08–6.63] vs. 0.56 [0.19–6.48], P = 0.02). The same was true also in the cART+LD− group (P = 0.04). Expression of *CD68* mRNA did not differ between the study groups in either adipose tissue depot (data not shown).

DISCUSSION

Herein we compared in detail the dorsocervical adipose tissue of cART-treated patients with and without lipodystrophy to the abdominal subcutaneous adipose tissue from

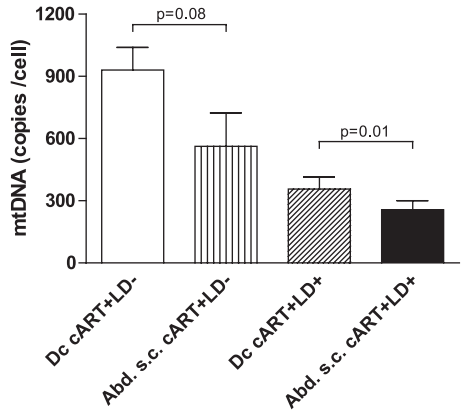

FIG. 1. Number of mtDNA copies per cell in dorsocervical (Dc) and abdominal subcutaneous (Abd. s.c.) adipose tissue of cART+LD+ and cART+LD− patients. Data are given as mean ± SEM.

the same individuals. Composition and characteristics of these two depots are of interest since in lipodystrophic patients one atrophies (abdominal depot), whereas the other is spared (dorsocervical depot).

mtDNA. We found that mtDNA copy numbers are significantly lower in the dorsocervical and the abdominal subcutaneous adipose tissue of the cART+LD+ group than in the respective depots in the cART+LD− group. Dorsocervical adipose tissue had significantly more mtDNA than the abdominal subcutaneous adipose tissue in the cART+LD+ group and almost significantly (P = 0.08) in the cART+LD− group. These results confirm previous reports on mtDNA depletion in lipoatrophic adipose tissue (14,20,30,31). However, the fact that mtDNA content is highly significantly lower (by 62%) also in the dorsocervical adipose tissue

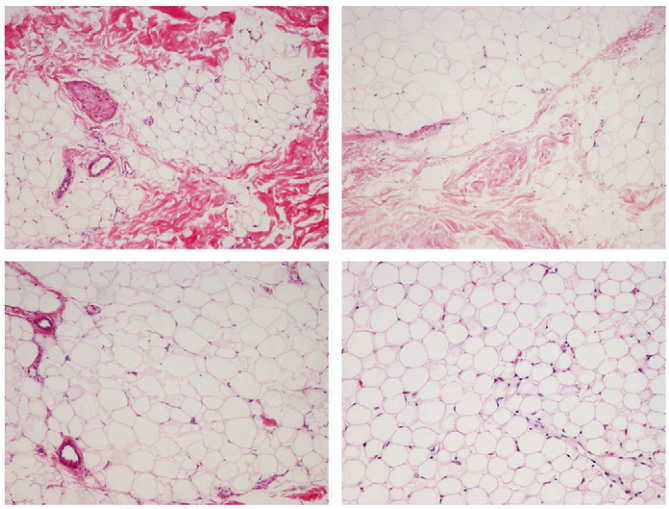

FIG. 2. Representative hematoxylin and eosin staining of the dorsocervical (*top panels*) and the abdominal (*bottom panels*) subcutaneous adipose tissue from cART+LD+ subjects (*left panels*) and cART+LD− subjects (*right panels*). Original magnification ×150. The dorsocervical adipose tissue exhibits less adipocytes surrounded by more prominent connective tissue than the abdominal subcutaneous adipose tissue. Note the regular structure of both the dorsocervical and the abdominal subcutaneous adipose tissue in the cART+LD− subjects—adipocytes are predominantly equal in size with few blood vessels observed between them. The adipose tissue from the cART+LD+ subjects, in contrast, tends to show greater cell size variation and more proliferated vascularization, although these differences do not reach statistical significance in our analyses. (A high-quality digital representation of this figure is available in the online issue.)

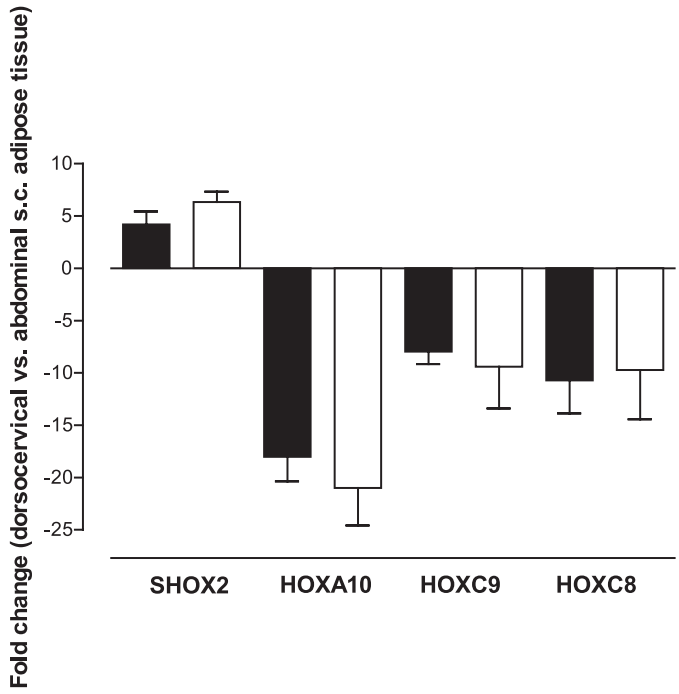

FIG. 3. Mean fold change in mRNA expression (measured by RT-PCR) in dorsocervical vs. abdominal subcutaneous adipose tissue in cART+LD+ group (black bars) and cART+LD− group (white bars). Positive values on the *y*-axis indicate upregulation and negative values indicate downregulation of the gene in question in the dorsocervical vs. abdominal subcutaneous adipose tissue. Error bars, SEM.

of cART+LD+ compared with the corresponding tissue in cART+LD− while the two depots are phenotypically comparable contradicts the prevailing theory that mtDNA depletion causes lipoatrophy. It also implies that once the lipodystrophy syndrome develops, the derangements observed in the adipose tissue are systemic and not restricted to atrophic abdominal subcutaneous adipose tissue.

Dorsocervical adipose tissue in the lipodystrophy syndrome has been suggested to represent BAT based on its anatomical location (14,32). Hallmarks of BAT include ample mitochondria featuring high metabolic activity and high expression of UCP1 (10–12). Previous studies reported significant amounts of *UCP1* mRNA in the buffalo hump, but not in healthy or lipoatrophic abdominal subcutaneous adipose tissue (14,15). Protein levels of UCP1 were not quantified. In our dorsocervical adipose tissue samples, we did not find increased copy numbers of mtDNA compared with abdominal subcutaneous adipose tissue and found no evidence of biologically significant *UCP1* expression using the same assay as previously used to verify the presence of *UCP1* in BAT in human supraclavicular adipose tissue studied by PET (18). Moreover, we did not see typical BAT morphology in our dorsocervical tissue samples, even in those from the clinically most prominent buffalo humps. This is in line with a recent study in subjects with cART-associated lipodystrophy reporting their dorsocervical adipose tissue to lack BAT morphology and not to be activated by cold exposure like true BAT would (19). Thus the present data support the view that dorsocervical adipose tissue in cART-associated lipodystrophy is not BAT.

Histology. Lipoatrophic adipose tissue, as compared with nonlipodystrophic adipose tissue, is known to be characterized by smaller adipocytes, greater cell size variation, disruption of cell membranes, and signs of

apoptosis as determined by immunohistochemistry staining compared with nonlipodystrophic adipose tissue (33–35). In our histological analyses, irrespective of the lipodystrophy status, we found less adipocytes and more connective tissue in the dorsocervical than in the abdominal subcutaneous adipose tissue. Thus these characteristics seem to be intrinsic to the dorsocervical location. Hitherto, light microscopy and ultrastructural characteristic data of adipose tissue from lipohypertrophic areas of HIV-1–infected subjects on cART have only been examined in one small study ($n = 4$) (35). Although the study did not specify the anatomical location of the lipohypertrophic areas, adipose tissue from these was reported to show similar, although milder, changes than those seen in lipoatrophic areas (35). These could not be quantitated because of the small sample size. The volume fraction of adipocytes and connective tissue was not reported but the finding of lipohypertrophic fat to be more normal is in line with the present data on lower *CD68* expression and more preserved mtDNA copy number in the dorsocervical compared with the abdominal subcutaneous adipose tissue (vide infra).

Inflammation. We found expression of *CD68* mRNA to be significantly lower in the dorsocervical than in the abdominal subcutaneous adipose tissue in both the cART+LD+ and the cART+LD− groups. Furthermore, microarray data suggested that genes involved in immune and inflammatory processes are downregulated in the dorsocervical as compared with the abdominal subcutaneous adipose tissue in the cART+LD+ group. These findings are in line with those of Guallar et al. (14), who found that inflammation, as judged from mRNA expression of *TNF-α* and *CD68*, is more severe in lipoatrophic abdominal subcutaneous adipose tissue than in the dorsocervical region, although in the latter study samples were not from the same subjects.

Homeobox genes. The microarray data suggested that dorsocervical and abdominal subcutaneous adipose tissue are largely similar. Using stringent criteria to avoid false-positive data, of all genes in the genome only less than 100 were differentially expressed. The genes differentially expressed in both the cART+LD+ and the cART+LD− groups are most likely to be those different because of the anatomic location of the tissues. The number of genes differentially expressed in the dorsocervical compared with the abdominal subcutaneous adipose tissue was markedly greater in the cART+LD+ than the cART+LD− group. Genes found to be discrepant between the dorsocervical and the abdominal subcutaneous depot only within the cART+LD+ group seem to represent characteristic features of lipoatrophy (e.g., upregulated inflammatory genes).

The foremost difference between dorsocervical and abdominal subcutaneous adipose tissue was in expression of the homeobox genes. The difference was observed in both the lipodystrophic and the nonlipodystrophic adipose tissue using microarray analysis and confirmed by real-time PCR. Homeobox genes are evolutionary highly conserved genes that serve as transcription factors guiding cells of the embryonal neural tube to migrate to their destined location and determining the distinctive traits inherit to the tissue being formed. There are four homeobox gene clusters in mammals: HOXA, HOXB, HOXC, and HOXD (36). Each cluster has several members numbered in ascending order starting from the anterior boundary of the central nervous system. Thus, the lower the order number of a homeobox gene, the more cranially it is located. Our findings are in line with this, since rostral *SHOX2* was overexpressed in dorsocervical compared with abdominal subcutaneous adipose tissue. The reverse was true for the caudal homeobox genes *HOXA10*, *HOXC9*, and *HOXC8*. These data support the validity of the microarray data and are in line with previous reports of depot-specific expression of homeobox genes in human adipose tissue in vivo (37–40) and in human adipose tissue–derived preadipocytes (41) and stromal cells (42). These differences were hypothesized to reflect the differentiation stages and adipogenic potential of adipose tissue depots as also suggested by work in murine models and cell cultures (43). The above human studies, however, evaluated expression of homeobox genes in adipose tissue samples from different locations along the ventrodorsal (subcutaneous–visceral–retroperitoneal) rather than the craniocaudal (dorsocervical–abdominal subcutaneous) axis that was examined in the current study. Of interest, HOXC4, which was expressed exclusively in BAT (37), was not differentially expressed between the two adipose tissue depots in the present microarray analysis. This fortifies the notion that dorsocervical adipose tissue in cART-associated lipodystrophy is not BAT.

We conclude that mtDNA is highly significantly lower (by 62%) even in the nonlipoatrophic dorsocervical adipose tissue of the cART+LD+ patients when compared with the corresponding depot of the cART+LD−. Therefore, mtDNA depletion does not seem to lead to lipoatrophy. In lipodystrophic patients, the dorsocervical adipose tissue is less inflamed than the lipoatrophic abdominal subcutaneous adipose tissue. It does not resemble BAT. The most marked difference in gene expression between dorsocervical and abdominal subcutaneous adipose tissue, irrespective of the lipodystrophy status, lay in expression of homeobox genes involved in organogenesis and regionalization. Disparate expression of such fundamental regulators of transcription might ultimately contribute to different patterns of differentiation and affect the susceptibility of the adipose tissue depot to cART-induced toxicity, perhaps making the abdominal subcutaneous depot more vulnerable to atrophy.

ACKNOWLEDGMENTS

This study was supported by grants from EVO and Sigrid Juselius Foundations (to H.Y.-J.), Orion Research Foundation (to K.S.), Lilly Foundation (to K.S.), Biomedicum Foundation (to K.S.), Finnish Medical Foundation (to K.S.), Jalmari and Rauha Ahokas Foundation, and Alfred Kordelin Foundation (to K.S.). No other potential conflicts of interest relevant to this article were reported.

K.S. and J.S. researched data, contributed to discussion, and wrote the manuscript. D.G., M.S., K.S., J.P., V.M.O., D.W., M.E.L., S.E., P.E., U.A.W., P.A., and M.R. researched data, contributed to discussion, and reviewed and edited the final version of the manuscript. H.Y.-J. researched data, contributed to discussion, and wrote the manuscript.

The authors thank Katja Sohlo and Mia Urjansson (Helsinki University Central Hospital, Department of Medicine) as well as Pentti Pölönen (Helsinki University Central Hospital, Department of Radiology) for skilful technical assistance and thank Antti Hakkarainen (Helsinki University Central Hospital, Department of Radiology) for useful discussions.

REFERENCES

1. Grinspoon S, Carr A. Cardiovascular risk and body-fat abnormalities in HIV-infected adults. N Engl J Med 2005;352:48–62

2. Caron-Debarle M, Lagathu C, Boccara F, Vigouroux C, Capeau J. HIV-associated lipodystrophy: from fat injury to premature aging. Trends Mol Med 2010;16:218–229
3. Mallewa JE, Wilkins E, Vilar J, et al. HIV-associated lipodystrophy: a review of underlying mechanisms and therapeutic options. J Antimicrob Chemother 2008;62:648–660
4. Villarroya F Domingo P, Giralt M. Drug-induced lipotoxicity: lipodystrophy associated with HIV-1 infection and antiretroviral treatment. Biochim Biophys Acta 2010;1801:392–399
5. Mallon PW, Wand H, Law M, Miller J, Cooper DA, Carr A; HIV Lipodystrophy Case Definition Study; Australian Lipodystrophy Prevalence Survey Investigators. Buffalo hump seen in HIV-associated lipodystrophy is associated with hyperinsulinemia but not dyslipidemia. J Acquir Immune Defic Syndr 2005;38:156–162
6. Grunfeld C, Rimland D, Gibert CL, et al. Association of upper trunk and visceral adipose tissue volume with insulin resistance in control and HIV-infected subjects in the FRAM study. J Acquir Immune Defic Syndr 2007; 46:283–290
7. Dixon JB, O'Brien PE. Neck circumference a good predictor of raised insulin and free androgen index in obese premenopausal women: changes with weight loss. Clin Endocrinol (Oxf) 2002;57:769–778
8. Laakso M, Matilainen V, Keinänen-Kiukaanniemi S. Association of neck circumference with insulin resistance-related factors. Int J Obes Relat Metab Disord 2002;26:873–875
9. Thamer C, Machann J, Staiger H, et al. Interscapular fat is strongly associated with insulin resistance. J Clin Endocrinol Metab 2010;95:4736–4742
10. Cannon B, Nedergaard J. Brown adipose tissue: function and physiological significance. Physiol Rev 2004;84:277–359
11. Cinti S. The adipose organ. Prostaglandins Leukot Essent Fatty Acids 2005; 73:9–15
12. Nedergaard J, Golozoubova V, Matthias A, et al. Life without UCP1: mitochondrial, cellular and organismal characteristics of the UCP1-ablated mice. Biochem Soc Trans 2001;29:756–763
13. Golozoubova V, Hohtola E, Matthias A, Jacobsson A, Cannon B, Nedergaard J. Only UCP1 can mediate adaptive nonshivering thermogenesis in the cold. FASEB J 2001;15:2048–2050
14. Guallar JP, Gallego-Escuredo JM, Domingo JC, et al. Differential gene expression indicates that 'buffalo hump' is a distinct adipose tissue disturbance in HIV-1-associated lipodystrophy. AIDS 2008;22:575–584
15. Rodríguez de la Concepción ML, Domingo JC, Domingo P, Giralt M, Villarroya F. Uncoupling protein 1 gene expression implicates brown adipocytes in highly active antiretroviral therapy-associated lipomatosis. AIDS 2004;18:959–960
16. Cypess AM, Lehman S, Williams G, et al. Identification and importance of brown adipose tissue in adult humans. N Engl J Med 2009;360:1509–1517
17. van Marken Lichtenbelt WD, Vanhommerig JW, Smulders NM, et al. Cold-activated brown adipose tissue in healthy men. N Engl J Med 2009;360: 1500–1508
18. Virtanen KA, Lidell ME, Orava J, et al. Functional brown adipose tissue in healthy adults. N Engl J Med 2009;360:1518–1525
19. Enerbäck S, Nuutila P, Oksi J. The importance of brown adipose tissue. N Engl J Med 2009;361:420–421
20. Sievers M, Walker UA, Sevastianova K, et al. Gene expression and immunohistochemistry in adipose tissue of HIV type 1-infected patients with nucleoside analogue reverse-transcriptase inhibitor-associated lipoatrophy. J Infect Dis 2009;200:252–262
21. Sutinen J, Walker UA, Sevastianova K, et al. Uridine supplementation for the treatment of antiretroviral therapy-associated lipoatrophy: a randomized, double-blind, placebo-controlled trial. Antivir Ther 2007;12:97–105
22. Huang W, Sherman BT, Tan Q, et al. The DAVID Gene Functional Classification Tool: a novel biological module-centric algorithm to functionally analyze large gene lists. Genome Biol 2007;8:R183
23. Silver N, Best S, Jiang J, Thein SL. Selection of housekeeping genes for gene expression studies in human reticulocytes using real-time PCR. BMC Mol Biol 2006;7:33
24. Pfaffl MW. A new mathematical model for relative quantification in real-time RT-PCR. Nucleic Acids Res 2001;29:e45
25. Yki-Järvinen H, Koivisto VA. Effects of body composition on insulin sensitivity. Diabetes 1983;32:965–969
26. Sutinen J, Häkkinen AM, Westerbacka J, et al. Rosiglitazone in the treatment of HAART-associated lipodystrophy—a randomized double-blind placebo-controlled study. Antivir Ther 2003;8:199–207
27. Sutinen J, Häkkinen AM, Westerbacka J, et al. Increased fat accumulation in the liver in HIV-infected patients with antiretroviral therapy-associated lipodystrophy. AIDS 2002;16:2183–2193
28. Friedewald WT, Levy RI, Fredrickson DS. Estimation of the concentration of low-density lipoprotein cholesterol in plasma, without use of the preparative ultracentrifuge. Clin Chem 1972;18:499–502
29. Matthews DR, Hosker JP, Rudenski AS, Naylor BA, Treacher DF, Turner RC. Homeostasis model assessment: insulin resistance and beta-cell function from fasting plasma glucose and insulin concentrations in man. Diabetologia 1985;28:412–419
30. Nolan D, Hammond E, Martin A, et al. Mitochondrial DNA depletion and morphologic changes in adipocytes associated with nucleoside reverse transcriptase inhibitor therapy. AIDS 2003;17:1329–1338
31. Walker UA, Bickel M, Lütke Volksbeck SI, et al. Evidence of nucleoside analogue reverse transcriptase inhibitor–associated genetic and structural defects of mitochondria in adipose tissue of HIV-infected patients. J Acquir Immune Defic Syndr 2002;29:117–121
32. Villarroya F, Domingo P, Giralt M. The importance of brown adipose tissue. N Engl J Med 2009;361:417–421
33. Domingo P, Matias-Guiu X, Pujol RM, et al. Subcutaneous adipocyte apoptosis in HIV-1 protease inhibitor-associated lipodystrophy. AIDS 1999;13: 2261–2267
34. Jan V, Cervera P, Maachi M, et al. Altered fat differentiation and adipocytokine expression are inter-related and linked to morphological changes and insulin resistance in HIV-1-infected lipodystrophic patients. Antivir Ther 2004;9:555–564
35. Lloreta J, Domingo P, Pujol RM, et al. Ultrastructural features of highly active antiretroviral therapy-associated partial lipodystrophy. Virchows Arch 2002;441:599–604
36. Shah N, Sukumar S. The Hox genes and their roles in oncogenesis. Nat Rev Cancer 2010;10:361–371
37. Cantile M, Procino A, D'Armiento M, Cindolo L, Cillo C. HOX gene network is involved in the transcriptional regulation of in vivo human adipogenesis. J Cell Physiol 2003;194:225–236
38. Gesta S, Blüher M, Yamamoto Y, et al. Evidence for a role of developmental genes in the origin of obesity and body fat distribution. Proc Natl Acad Sci USA 2006;103:6676–6681
39. Vohl MC, Sladek R, Robitaille J, et al. A survey of genes differentially expressed in subcutaneous and visceral adipose tissue in men. Obes Res 2004;12:1217–1222
40. Dankel SN, Fadnes DJ, Stavrum AK, et al. Switch from stress response to homeobox transcription factors in adipose tissue after profound fat loss. PLoS ONE 2010;5:e11033
41. Tchkonia T, Lenburg M, Thomou T, et al. Identification of depot-specific human fat cell progenitors through distinct expression profiles and developmental gene patterns. Am J Physiol Endocrinol Metab 2007;292: E298–E307
42. Levi B, James AW, Glotzbach JP, Wan DC, Commons GW, Longaker MT. Depot-specific variation in the osteogenic and adipogenic potential of human adipose-derived stromal cells. Plast Reconstr Surg 2010;126:822–834
43. Cowherd RM, Lyle RE, Miller CP, Mcgehee RE Jr. Developmental profile of homeobox gene expression during 3T3-L1 adipogenesis. Biochem Biophys Res Commun 1997;237:470–475